JOURNAL OF MATERIALS SCIENCE **38** (2003) 4507–4522

Effect of solution heat treatment and additives on the microstructure of Al-Si (A413.1) automotive alloys

M. A. MOUSTAFA
Central Metallurgical Research and Development Institute, Helwan, Cairo, Egypt; Département des sciences appliquées, Université du Québec à Chicoutimi, Chicoutimi, Québec, Canada G7H 2B1

F. H. SAMUEL
Département des sciences appliquées, Université du Québec à Chicoutimi, Chicoutimi, Québec, Canada G7H 2B1
E-mail: fhsamuel@uqac.ca

H. W. DOTY
GM Powertrain Group, Metal Casting Technology Inc., Milford, NH 03055, USA

A study was carried out to determine the role of additives such as Mg, Cu, Be, Ag, Ni, and Zn on the microstructural characteristics of grain refined, Sr-modified eutectic A413.1 alloy (Al-11.7% Si) during solution heat treatment. For comparison purposes, some of the alloys were also studied in the non-modified condition. The alloys were cast in a steel permanent mold preheated at 425°C that provided a microstructure with an average dendrite arm spacing (DAS) of ~22 μm. Castings were solution heat treated at 500 ± 2°C for times up 24 h, followed by quenching in warm water (at 60°C). Microstructural analysis of the as-cast and heat-treated castings was carried out using optical microscopy in conjunction with image analysis. Phase identifications were done using the electron probe microanalysis (EPMA) technique.

In the as-cast condition, the addition of 0.42 wt% Mg to the unmodified alloy produced relatively large Si particles compared to the base A413.1 alloy. The Si particle size remained more or less the same with increase in solution treatment time and Mg level. Both Mg_2Si and Al_2Cu phases were observed to dissolve almost completely after 8 h solution time, while the $Al_5Cu_2Mg_8Si_6$ and α-$Al_{15}(Mn,Fe)_3Si_2$ phases were found to persist even after 24 h. The β-Al_5FeSi iron intermetallic platelets (possibly nucleated on SrO particles during solidification) underwent partial dissolution by the diffusion of Si atoms into the surrounding aluminum matrix after 24 h solution treatment. The presence of Ni and Cu (dissolved) in the α-Fe phase contributes to its stability during solution treatment. The modification effect of Sr on the β-Al_5FeSi platelets is intensified in the presence of Zn.

1. Introduction

The use of aluminum components in the automotive industry has increased considerably during the past ten years due to their lightweight and reduced fuel energy consumption advantages. Another advantage, which is equally important from an environmental point of view, is the fact that aluminum components may be recycled at relatively low energy costs. Among aluminum alloys, aluminum-silicon (Al-Si) alloys are known for their good castability and mechanical properties. The addition of Mg, Cu, and Zn makes the alloys heat-treatable [1, 2], providing the means to enhance their properties with the use of appropriate heat treatments. The mechanical properties of an Al-Si cast alloy are mainly determined by its cast structure and the microstructural characteristics such as the grain size, dendrite arm spacing (DAS), the size, shape and distribution of the eutectic silicon particles, as well as the morphologies and amounts of intermetallic phases present [3, 4]. These parameters are completely changed after heat treatment [5, 6], which, in turn, influences the resultant mechanical properties [7, 8].

The present work was undertaken to investigate the effect of the addition of various elements viz., Mg, Cu, Be, Ag, Ni and Zn on changes in the eutectic Si particle characteristics as well as the changes in the microstructure following solution heat treatment at 500°C for times up to 24 h.

TABLE I Chemical compositions of the alloys used in the present work

	Chemical composition (wt%)												
Alloy code	Si	Fe	Cu	Mn	Mg	Cr	Ni	Zn	B	Be	Sr	Ag	Ti
M0[a]	11.90	.88	.875	.210	.082	.017	.017	.340	.008	.000	.002	.000	.052
M1[b]	11.74	.793	.875	.211	.086	.026	.020	.338	.008	.000	**.030**	.000	.051
M2	11.79	.789	.867	.206	**.411**	.018	.019	.343	.007	.000	**.026**	.000	.050
M2N	11.46	.749	.878	.199	**.422**	.017	.023	.334	.007	.000	.000	.000	.050
M2B	11.72	.761	.867	.196	**.446**	.018	.024	.324	.007	**.018**	**.025**	.000	.051
M3	11.74	.800	**2.64**	.193	.070	.040	.022	.321	.008	.000	**.039**	.000	.051
M3N	11.76	.798	**2.66**	.195	.067	.040	.022	.331	.008	.000	.000	.000	.051
M4[c]	11.28	.751	**2.61**	.184	**.379**	.033	.027	.313	.007	.000	**.041**	.000	.052
M4N	11.28	.751	**2.61**	.184	**.379**	.033	.027	.313	.007	.000	.000	.000	.052
A	11.65	.722	**2.70**	.182	**.366**	.016	.030	.031	.009	.000	**.025**	**.715**	.050
AB	11.48	.720	**2.73**	.182	**.396**	.017	.032	.309	.009	**.016**	**.034**	**.710**	.050
1NN	11.86	.678	**2.46**	.200	**.314**	.018	**.627**	.241	.002	.000	.000	.000	.050
1N	11.86	.678	**2.46**	.200	**.314**	.018	**.627**	.241	.002	.000	**.021**	.000	.050
2N	11.88	.673	**2.43**	.192	**.378**	.020	**1.41**	.240	.002	.000	**.026**	.000	.050
Z	11.95	.706	**2.81**	.198	**.378**	.019	.029	**2.74**	.002	.000	**.020**	.000	.046
ZN	11.89	.677	**2.66**	.192	**.444**	.019	**.634**	**2.25**	.002	.000	**.021**	.000	.053

[a]Base A413.1 alloy.
[b,c]Reference alloys.

2. Experimental procedure

All the experiments were conducted on an A413.1 alloy (coded M0) that was received in the form of 12.5 kg ingots. Its chemical composition is shown in Table I. Measured amounts of alloying elements were added to the base alloy, viz., copper, magnesium, silver, nickel, zinc and beryllium. The experimental procedure involved the preparation of 40 kg melts using a SiC crucible heated in an electric resistance furnace. The melt temperature was kept at $725 \pm 5^{\circ}$C.

The alloying elements were added to the melt of M0 alloy in the form of master alloys. Only Mg was added in the form of a pure metal. All alloys were grain refined with TiB_2 (containing ~40 ppm B) and modified with 200–400 ppm Sr. In certain cases, for comparison purposes, the alloys were grain refined but not modified (viz., M2N, M3N, M4N, and 1NN alloys, see Table I). The alloys listed in Table I are grouped into three categories: (i) the base alloy, M0, (ii) alloys M1 through M3N, with M1 (viz., Sr-modified M0 alloy) representing the base or reference alloy for this group, and (iii) alloys M4 through ZN, having M4 as their reference alloy. All melts were degassed using argon and a rotating graphite degassing impeller (30 min at 125 rpm).

Microstructures of the as-cast and solution heat-treated samples at different solution heat treatment times (0, 8 and 24 h) were examined using optical microscopy and electron probe microanalysis (EMPA). The latter was coupled with energy dispersive X-ray (EDX) and wavelength dispersive spectroscopic (WDS) facilities, using a Jeol JXA-8900L WD/ED Combined Micro-analyzer, operating at 20 kV and 30 nA. The silicon particle characteristics were measured using a Leco 2001 image analyzer. From these, the following parameters were determined:

- Average Si particle area (μm^2) and its standard deviation;
- Average Si particle length (μm) and its standard deviation;
- Roundness ratio of Si particles (%), defined as $R = (4\pi A)/P^2 \times 100$, where $A = \pi R^2$, $P = 2\pi R$, and roundness =100 for a perfect circle (actually ~95%, because of the square matrix created by the pixels in the image analyzer);

TABLE II Silicon particle characteristics following different solution treatment times at 500°C

		Particle area (μm^2)		Particle length (μm)		Roundness ratio (%)		Aspect ratio		
Alloy code	Solution time (h)	Av.	SD	Av.	SD	Av.	SD	Av.	SD	Density (particles/mm^2)
M0	0[a]	6.39	19.08	4.71	5.54	60.75	28.80	2.71	1.50	21 045
	8	7.20	15.61	4.24	4.25	71.92	22.95	2.12	1.00	23 325
	24	10.96	20.88	5.30	5.00	72.06	22.33	2.11	1.07	14 187
M1	0[a]	0.64	3.51	1.20	1.06	77.32	21.39	1.91	0.77	167 799
	8	2.24	2.71	1.93	1.37	85.41	13.11	1.48	0.41	62 807
	24	3.41	3.95	2.31	1.67	85.43	12.20	1.48	0.40	41 809
M2N	0[a]	7.01	12.30	5.44	6.48	53.88	30.87	2.88	1.62	19 919
	8	9.05	12.02	5.18	4.63	65.17	23.82	2.35	1.19	20 480
	24	10.91	13.03	5.41	4.50	68.68	21.47	2.25	1.04	14 622

[a]As-cast condition; Av.: average; SD: Standard deviation.

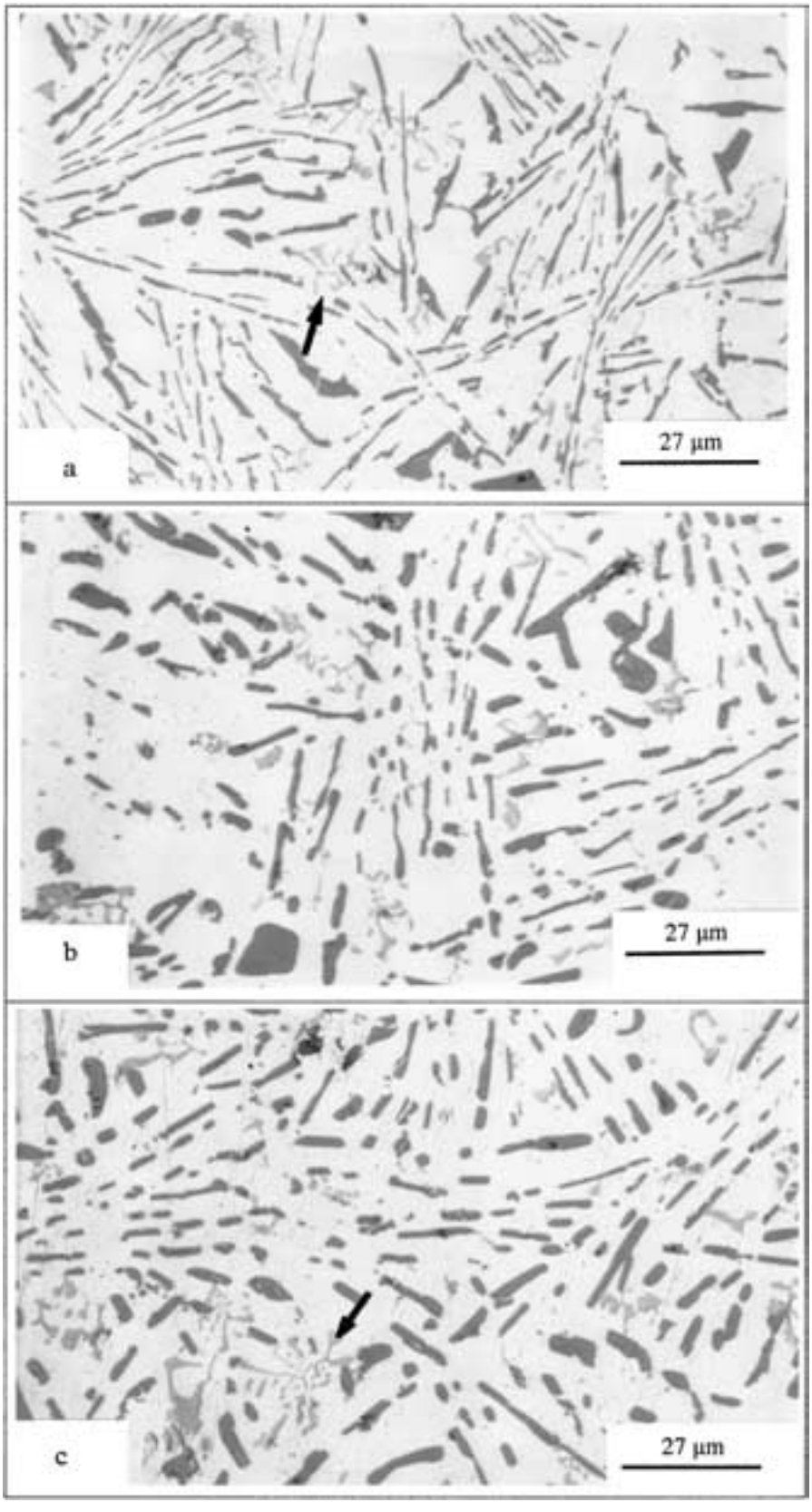

Figure 1 Optical micrographs showing the effect of solution treatment at 500°C on the Si morphology in unmodified A413.1 (M0) alloy: (a) 0 h, (b) 8 h, and (c) 24 h. Arrows point to α-Fe script particles.

- Aspect ratio: ratio of maximum to minimum dimensions of Si particles; and
- Density of Si particle count per unit area (number of particles/mm^2).

The measurements were carried out over fifty fields (such that the sample surface was traversed in a regular, systematic manner) at 200× or 500× magnification, depending on whether the alloy was unmodified or Sr-modified. Table II lists these parameters for some representative alloys (viz., M0, M1, M2N) and solution treatment times. The longitudinal sections beneath the fracture surfaces of some of the tensile-tested specimens (M1, M2N, M4, and

2N alloys) were also examined employing optical microscopy.

3. Results and discussion

3.1. Si particle characteristics

Particle size, shape, and spacing are the factors that characterize the silicon particle morphology. Under slow cooling conditions (cooling rate $<1^{\circ}$C/s), the Si particles are present as brittle, coarse acicular plates in the unmodified Al-Si alloys, as shown in Fig. 1a. These plates act as crack initiators and appreciably lower the alloy mechanical properties. Therefore, small amounts of a chemical modifier, i.e., Sr, were added to the alloy melts to change the Si morphology to the fibrous form upon solidification, as shown in Fig. 2a.

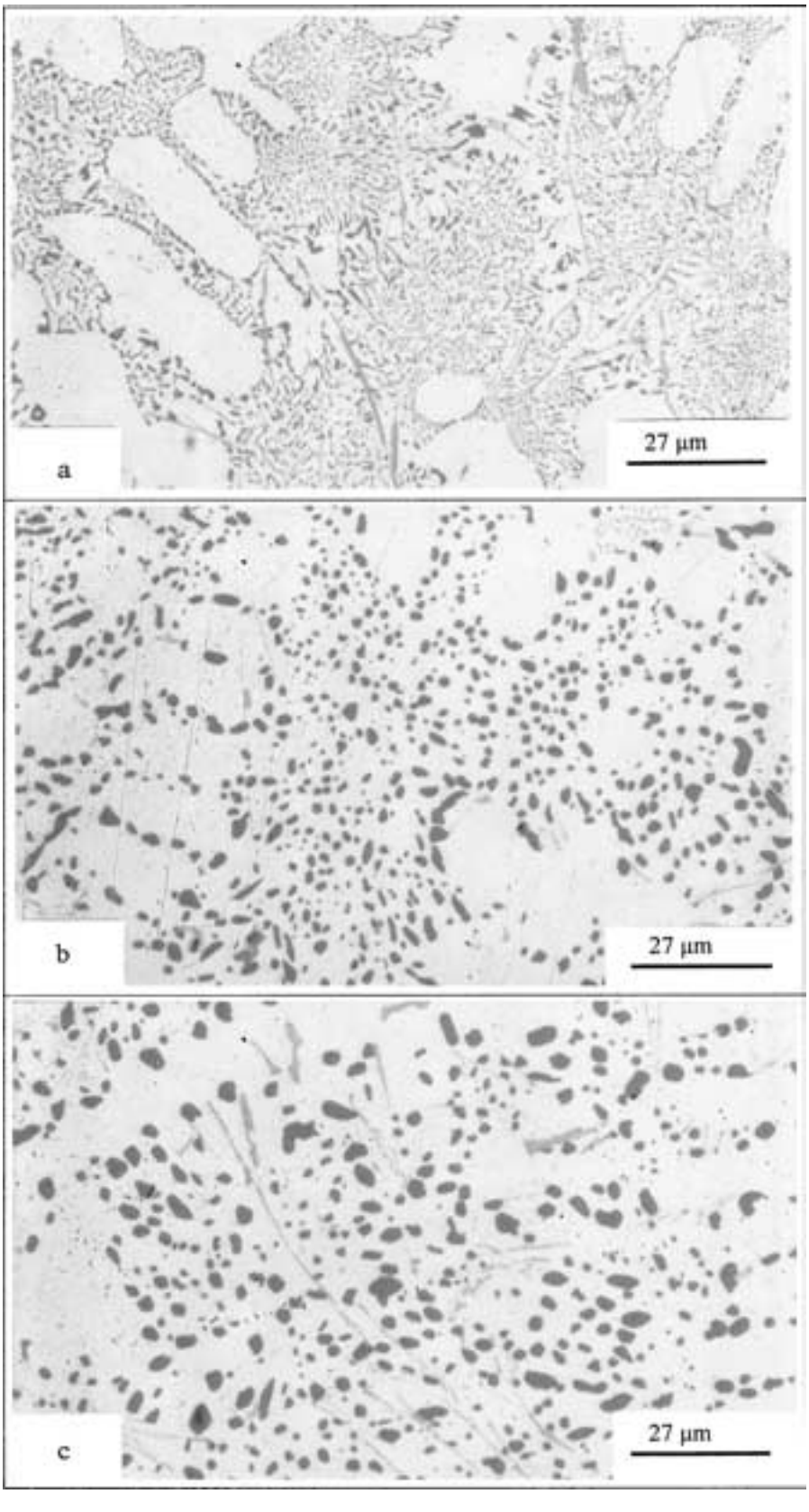

Figure 2 Optical micrographs showing the effect of solution treatment on the Si morphology in Sr-modified M1 alloy: (a) 0 h, (b) 8 h, and (c) 24 h.

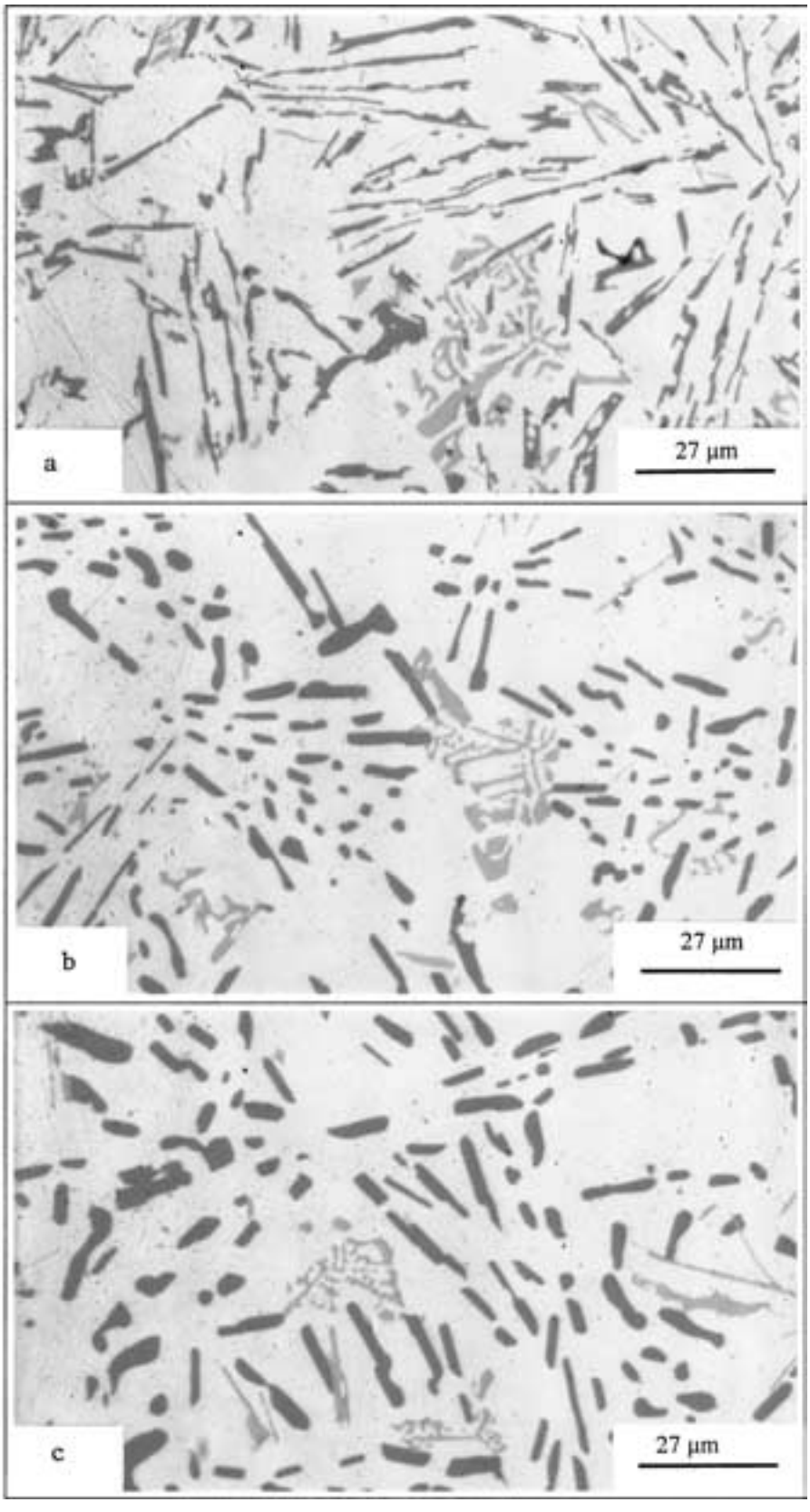

Figure 3 Optical micrographs showing the effect of solution treatment on the Si morphology in unmodified M2N alloy: (a) 0 h, (b) 8 h, and (c) 24 h.

Subjecting an unmodified or modified casting to a high temperature solution treatment for sufficiently long times can also alter the Si particle characteristics. Generally speaking, when the Al-Si alloys are solution treated at an elevated temperature (e.g., 500°C), after a certain period of time, shape perturbations in the silicon particles begin to arise until, ultimately, the particles are broken down into a series of spherical crystals. This process occurs because of the instability of the interfaces between two different phases and is driven by a reduction in the total interfacial energy. This stage is called the *fragmentation* or *spheroidization* stage.

Subsequently, the Si particle size begins to increase as a result of particle coarsening if its size is greater than the critical volume, whereas smaller particles dissolve according to Ostwald ripening [9]. This stage is termed the *coarsening* stage. In recent years, chemical and thermal modifications are being used in conjunction to produce the desired properties of a casting [10, 11].

Fig. 1 depicts the optical micrographs showing the effect of solution treatment at different times on the Si parameters of the unmodified base alloy (M0 alloy), while Table II lists the numerical values of these parameters. In the as-cast condition, the Si particles were platelets with an average length of 4.71 μm. These samples were cut from the tensile test bars cooled in a metallic mold (dendrite arm spacing $\sim$22 μm). The average length remained more or less unchanged (4.24 μm) after 8 h solution treatment at 500°C, whereas the Si particle density increased somewhat from 2.1×10^4 to 2.3×10^4 particles/mm^2, i.e., by about 11%. These results show that the Si platelets underwent partial fragmentation. The decrease in the aspect ratio from 2.71 to 2.12 supports this suggestion. When the solution time increased to 24 h, the average Si particle area, length, and roundness increased, while the aspect ratio and density decreased. The decrease in Si particle density (by $\sim$39%) may indicate the commencement of the coarsening process. The negligible decrease in aspect ratio ($\sim$0.3%) suggests the persistence of the platelet shape of the Si particles, as is also seen from Fig. 1c.

The micrographs in Fig. 2 illustrate the combined effect of Sr addition and solution treatment time on the eutectic Si particles in the M1 alloy. From Fig. 2a, it can be seen that the addition of $\sim$300 ppm Sr leads to full modification of the Si particles in the as-cast condition. As Table II shows, the average Si particle area, length, and aspect ratio of M1 alloy in the as-cast condition decreased respectively, by 90%, 75%, and $\sim$30% compared to M0 alloy, whereas, the average roundness and density increased by 27% and $\sim$700%, respectively. These parameters were further reduced after solution heat treatment (c.f. Fig. 2b and c with Fig. 1b and c). For example, after 24 h solution heat treatment at 500°C, the average Si particle area, length, and aspect ratio of M1 alloy decreased by $\sim$70%, 56%, and 30%, respectively,

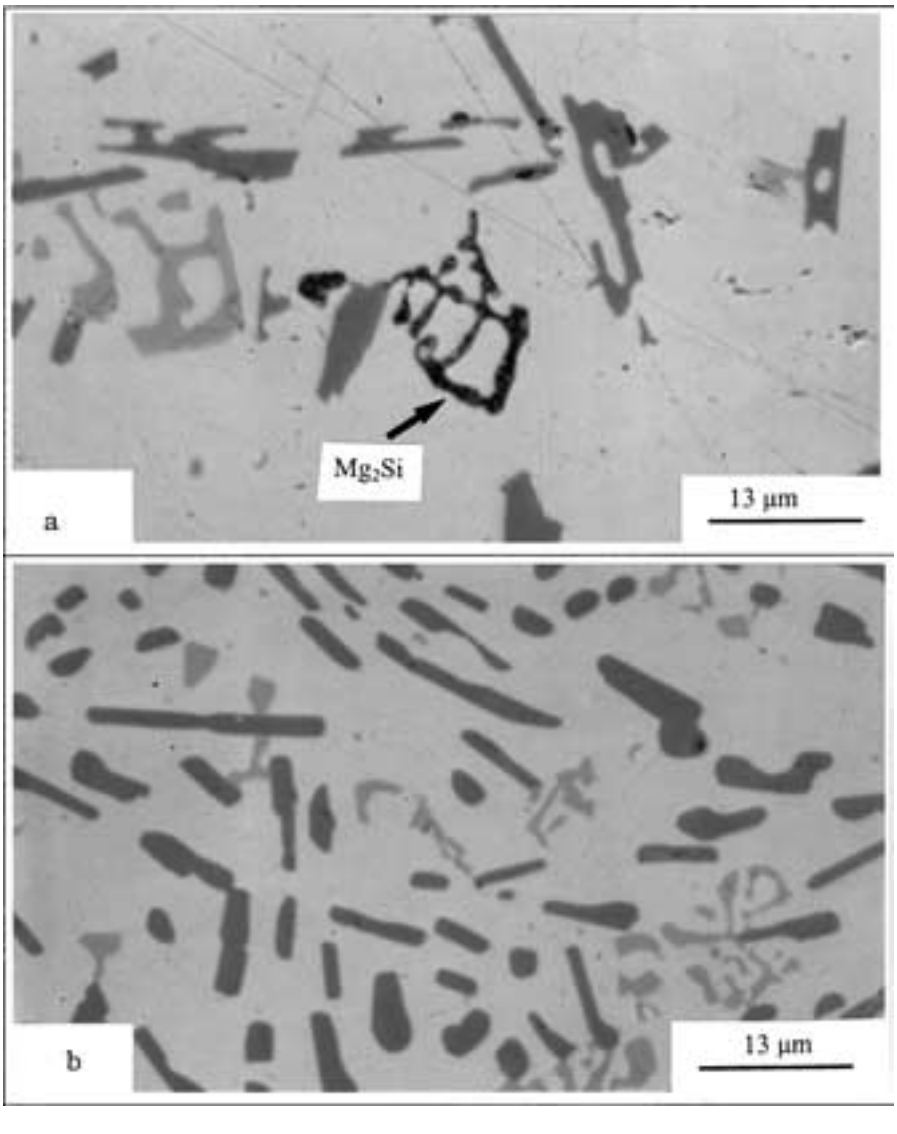

Figure 4 Optical micrographs showing dissolution of Mg_2Si phase particles in unmodified M2N alloy after solution treatment: (a) as-cast condition and (b) after solution treatment for 8 h at 500°C.

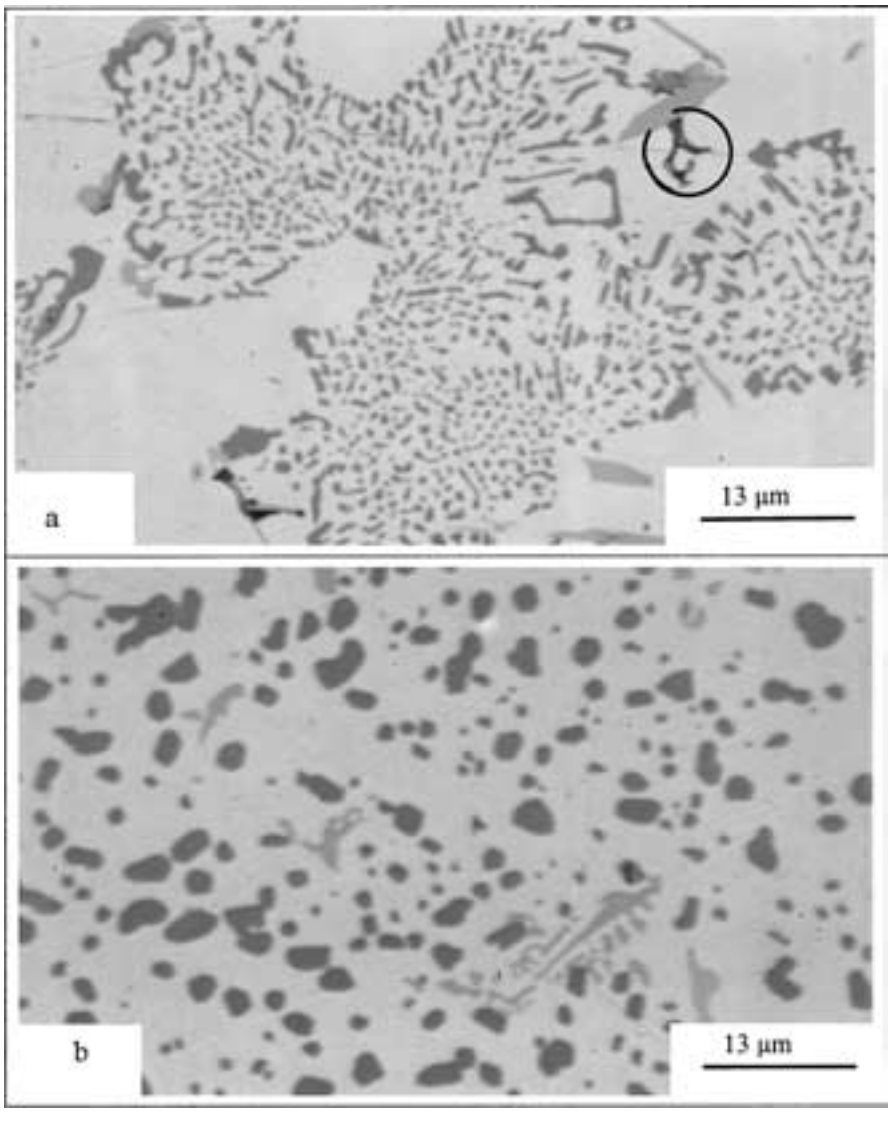

Figure 5 Optical micrographs showing dissolution of Mg_2Si phase particles in unmodified M2 alloy: (a) as-cast condition and (b) following solution heat treatment for 8 h at 500°C.

compared to M0 alloy (similarly treated), while the roundness, and particle density increased by 19% and ∼200%. These values shows that a combination of chemical modification and solution heat treatment ameliorate the Si particle characteristics much more effectively than does solution heat treatment alone, even after prolonged solution treatment times (24 h at 500°C).

When 0.42% Mg was added to the unmodified base alloy, i.e., M2N alloy, the eutectic Si morphology or size did not exhibit any significant change. Fig. 3 shows the variation in the Si parameters as a function of solution time at 500°C. As can be seen from Table II, the average Si particle area length, and aspect ratio of M2N alloy in the as-cast condition were marginally increased by ∼10%, 15%, and 6.5%, respectively, with a corresponding decrease in the average roundness and particle density of ∼11%, and ∼5%, respectively, compared to the as-cast base M0 alloy. These observations are in agreement with the findings of Wang and Caceres [11], who reported that a higher Mg content (0.4% and 0.66%) resulted in large Si particles and flakes in unmodified Al-Si-Mg alloys. After solution heat treatment for 24 h at 500°C, the average Si particle area length, aspect ratio, roundness, and density varied slightly, by about −0.5%, 2%, 6.5%, −5% and 3%, respectively. Taking into account the experimental error and the standard deviation values listed in Table II, it can be concluded that Mg does not affect the transformation of the Si particles during solution treatment. In other words, the fragmentation and spheroidization processes remain practically unaffected by the presence of 0.42% Mg.

In a previous publication, the authors [12] reported on the partial refinement of the eutectic Si particles in the presence of 0.4% Mg, when the alloy was cooled at ∼0.8°C/s. Thus, it may be reasonable to suggest that the modification effect of Mg is more noticeable at low solidification rates, rather than at the relatively high cooling rate (i.e., metallic mold) employed in the present case. It is worth noting in Table II that the average Si particle length decreased in the unmodified M0 and M2N alloys after 8 h solution treatment (from 5.54 μm and 6.48 μm to 4.25 μm and 4.63 μm, respectively), indicating the progress of fragmentation. After 24 h solution treatment, however, the Si particle lengths

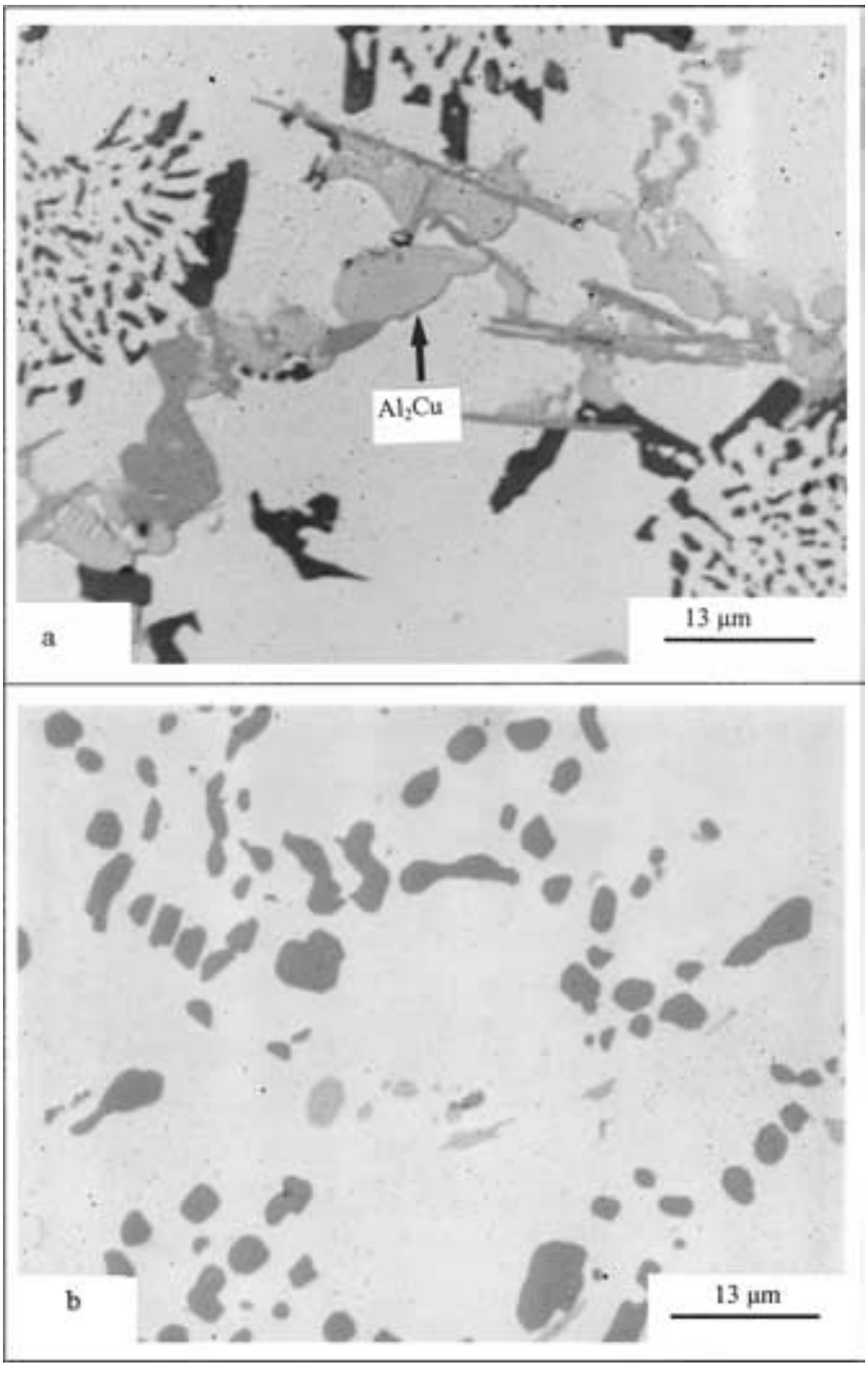

Figure 6 Optical micrographs showing the complete dissolution of Al_2Cu phase during solution treatment of M3 alloy: (a) as-cast condition and (b) following solution heat treatment for 8 h at 500°C.

increased again, corresponding to the coarsening stage. In contrast, the fragmentation stage was completed in the Sr-modified M1 alloy within 8 h of solution treatment (or possibly less).

In their study on heat treatment of cast Al-Si-Mg alloys, Apelian *et al.* [6] have reported that the Si particles undergo spheroidization and coarsening during solution treatment. The rate of spheroidization is extremely rapid in modified alloys, while only a small fraction of Si particles are spheroidzed even after 10 to 15 h solution treatment in the unmodified case. Due to the large differences in particle size distribution, however, the driving force for coarsening is greater in the unmodified than in the modified alloys. Consequently, the unmodified alloys exhibit a higher coarsening rate.

3.2. Intermetallic phases

3.2.1. Mg_2Si phase

Dissolution of Mg_2Si particles depends on the solution temperature and time. The solubility of Mg and Si in the Al-matrix increases with the temperature [6, 9, 13]. Homogenization to minimize segregation of alloying elements in an aluminum casting is determined by the solution temperature and by the dendrite arm spacing of the cast microstructure. As mentioned previously, the dendrite arm spacing was $\sim$22 μm in the present work,

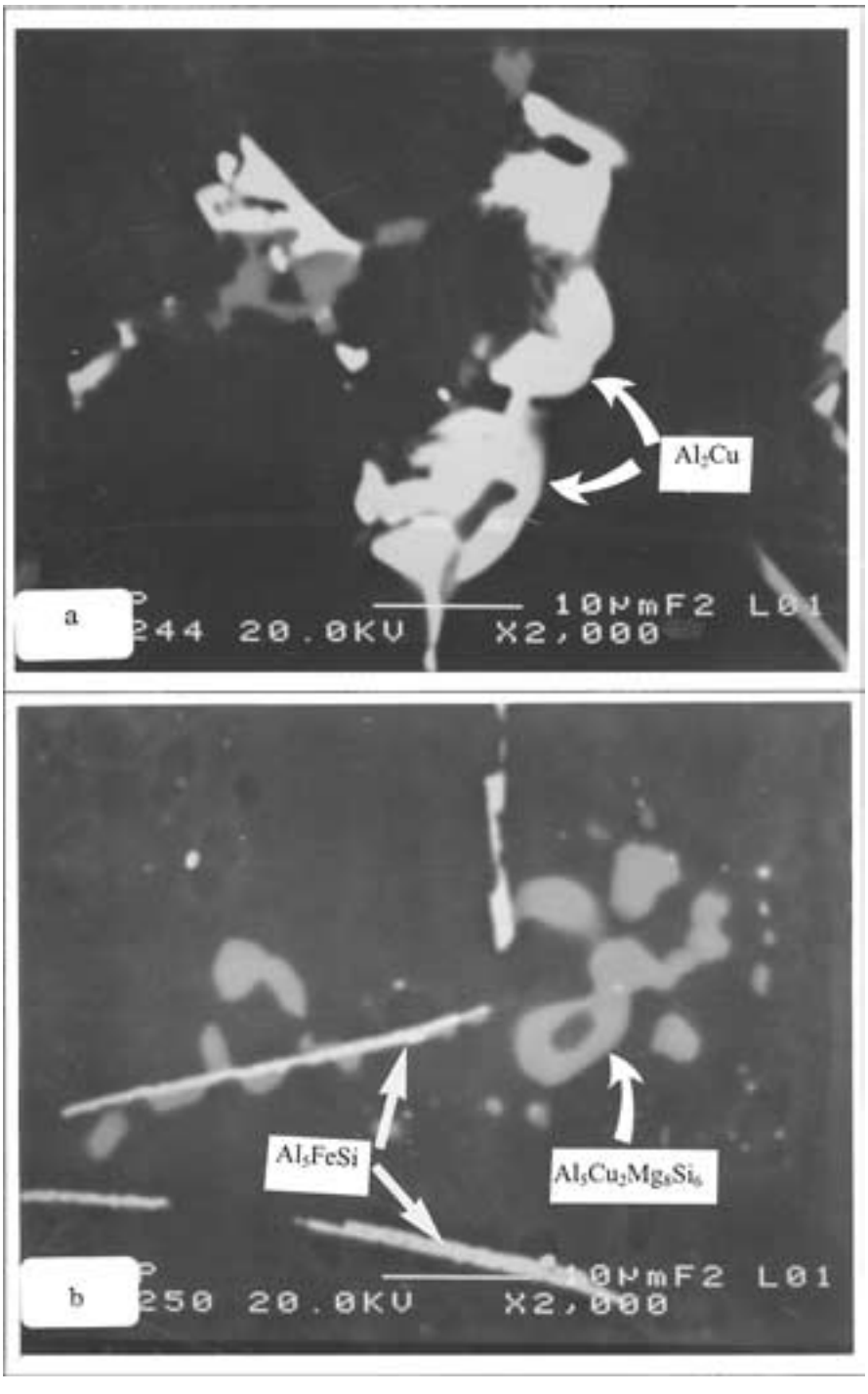

Figure 7 High magnification backscattered images obtained from M4 alloy showing the presence of Al_2Cu and $Al_5Cu_2Mg_8Si_6$ phase particles in: (a) the as-cast condition and (b) after 24 h solution heat treatment at 500°C.

and the solution temperature was kept at 500 ± 2°C. This temperature was selected to be as close as possible to the $Al_5Mg_8Cu_2Si_6$ phase precipitation temperature in order to obtain the maximum concentration of Mg in solid solution, without causing incipient melting of the Cu-containing phases. According to Mondolfo [14], the maximum solubility of Mg in Al-Si alloys at 500°C (under equilibrium conditions) is ∼0.52%, which is much higher than the percentage of Mg used in the present work (Table I).

The microstructures of the two Mg-containing alloys (M2N and M2 alloys) were examined using optical microscopy. Figs 4 and 5 are the micrographs of the unmodified M2N alloy and modified M2 alloy, in the as-cast and 8 h/500°C conditions. As can be seen from Fig. 4a, the Mg_2Si phase precipitates in the form of large Chinese script particles in the unmodified alloy. Addition of 260 ppm Sr resulted in modifying both the eutectic Si and Mg_2Si phase particles, as shown in Fig. 5a. When these two alloys were solution heat-treated for 8 h at 500°C, complete dissolution of the Mg_2Si took place, regardless of its original shape or size, as shown in Figs 4b and 5b. It should also be noted that the Si particles in Fig. 5b corresponding to M2 alloy are relatively larger than those viewed in Fig. 2b for M1 alloy where no Mg was added.

3.2.2. Al_2Cu phase

This phase precipitates during solidification in different forms (i.e., block-like, eutectic or as a mixture of both types) depending on the cooling rate and the modification conditions [15, 16]. The Al_2Cu phase has a low melting temperature [17]. Sokolowski *et al.* [18] reported that the copper-rich phase in as-cast Al-Si-Cu alloys causes localized melting once the solution treatment temperature reaches 495°C, thus limiting the conventional single-stage solution treatment. Therefore, the solution temperature must be lower than the melting point of Al_2Cu in order to avoid any incipient melting [19, 20]. Another method recommended to overcome this problem consists of a two-stage solution treatment whereby the conventional solution treatment is followed by a second solution treatment at a temperature above 495°C [21]. Fig. 6a shows the presence of the Al_2Cu phase in the Sr-modified M3 alloy in the as-cast condition, whereas Fig. 6b reveals almost complete dissolution of the phase after solution treatment for 8 h at 500°C. The arrow in Fig. 6b points to the traces of undissolved Al_2Cu particles.

3.2.3. Al-Cu-Mg-Si phases

In Al-Si-Cu-Mg systems, precipitation of $Al_5Cu_2Mg_8Si_6$ is reported to take place at the end of the Al-Al_2Cu eutectic reaction [22]. Its formation temperature and shape are mainly related to the concentration of Mg as well as the applied cooling rate. In most cases, this phase appears in the form of small particles growing out of Al_2Cu particle clusters, as shown in Fig. 7a, which shows the microstructure of M4 alloy in the as-cast condition. It is interesting to observe the persistence of this phase after 24 h solution heat treatment, as shown in Fig. 7b.

The corresponding EDX spectra for the Al_2Cu and $Al_5Cu_2Mg_8Si_6$ phases are shown in Fig. 8a and b, respectively. The WDS analysis obtained from the latter was close to $Al_5Cu_2Mg_7Si_5$. This difference may be attributed to the fact that the $Al_5Cu_2Mg_8Si_6$ particles are relatively thin, which would allow more aluminum from the matrix to be acquired during analysis. It should be mentioned here that the WDS analysis of these particles revealed unexpectedly higher concentrations of aluminum than reported for the as-cast condition. This observation may indirectly indicate the sluggish dissolution (or thinning) of the $Al_5Cu_2Mg_8Si_6$ phase during solution heat treatment, even though its formation temperature is approximately 2°C above the solution temperature used in the present work. Thus, any increase in the solution temperature would definitely lead to incipient melting of the phase.

3.2.4. Fe-intermetallic phases

The presence of iron as an impurity in Al-Si alloys leads to precipitation of different iron intermetallics with various morphologies, some of which can have a deleterious effect on the alloy mechanical properties. The two main iron intermetallics observed are the α-$Al_{15}(MnFe)_3Si_2$ and β-Al_5FeSi phases (subsequently denoted as α-Fe and β-Fe).

3.2.4.1. α-Fe phase. The α-$Al_{15}(MnFe)_3Si_2$ iron intermetallic occurs in the form of Chinese script. The size and distribution of this phase during solidification is strongly related to the amount of Sr added to the alloy.

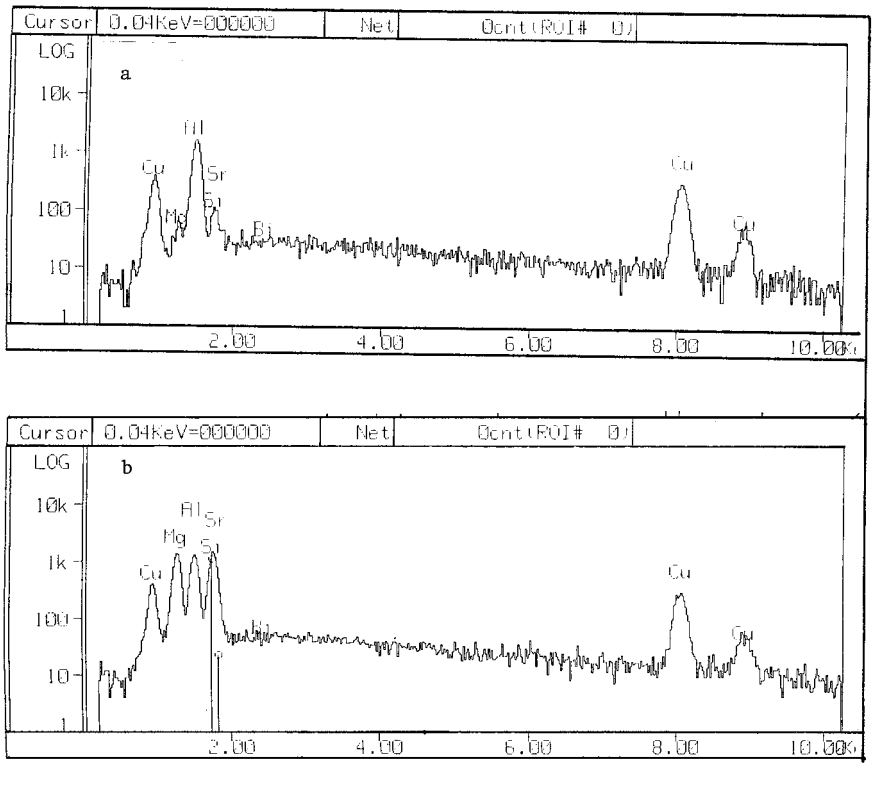

Figure 8 EDX spectra corresponding to (a) Al_2Cu phase and (b) $Al_5Cu_2Mg_8Si_6$ phase shown in Fig. 7.

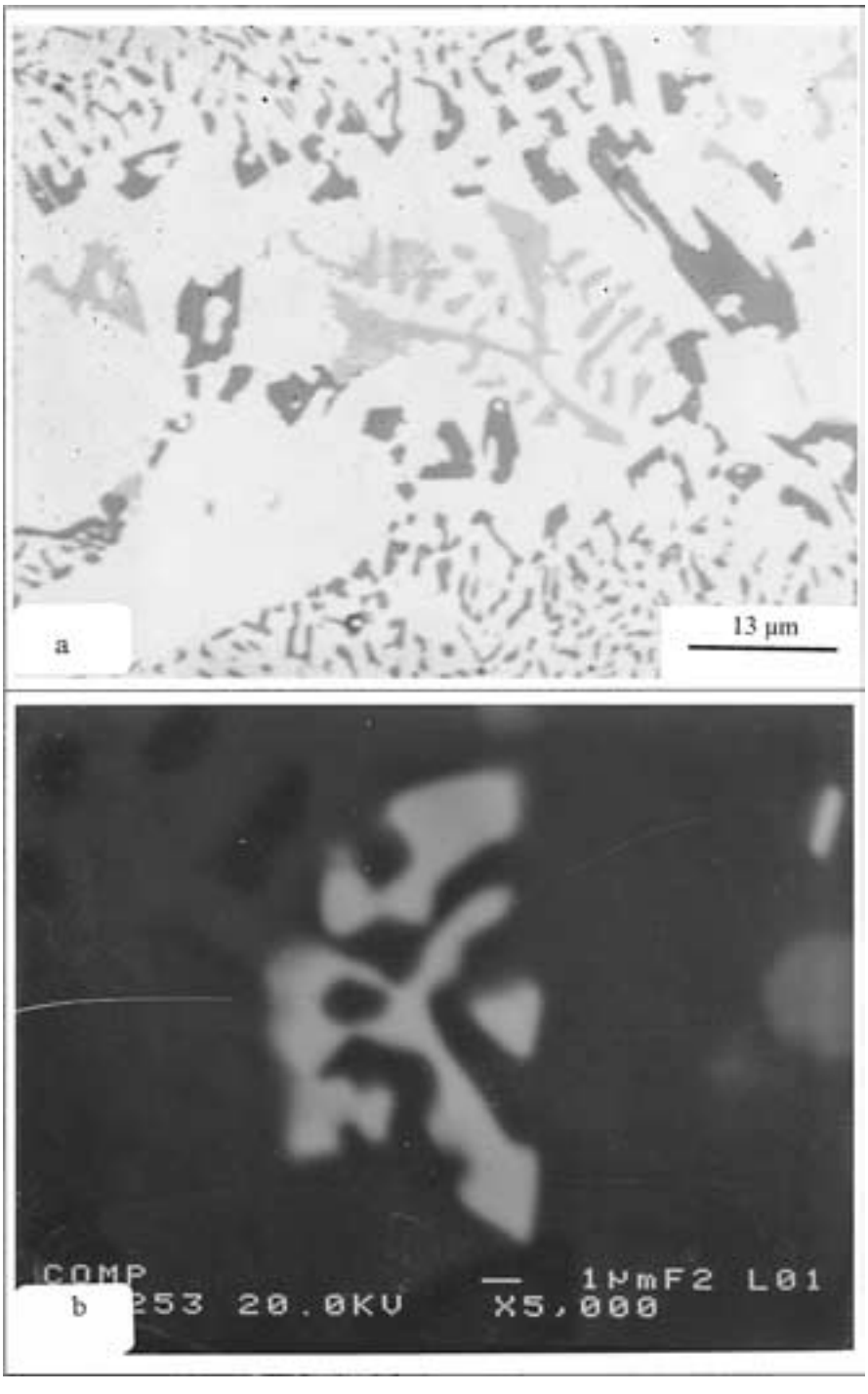

Figure 9 Morphology of α-$Al_{15}(MnFe)_3Si_2$ phase observed in M1 alloy: (a) as-cast condition, optical micrograph and (b) after 24 h solution treatment at 500°C, backscattered image.

In the unmodified alloy, the α-Fe phase precipitates in the interdendritic regions, along with the eutectic silicon. However, with the addition of Sr, the α-Fe phase precipitates prior to the formation of the α-Al dendritic network, as exemplified in Fig. 9a for the M1 alloy in the as-cast condition. The reason for such a dramatic change in the mechanism of the precipitation of this phase, i.e., from small interdendritic particles (arrowed in Fig. 1a and c) in the unmodified M0 alloy to the large predendritic particles in the Sr-modified case (M1 alloy, Fig. 9a) is not yet clearly understood. As previously documented [12], the solubility of this phase during solution heat treatment is almost nil. In confirmation with these observations, Fig. 9b shows the presence of the α-Fe phase in M1 alloy after solution treatment for 24 h at 500°C, showing no noticeable changes compared to the particle shown in Fig. 9a.

3.2.4.2. β-Fe phase. In contrast to the α-Fe phase which remains unchanged during solution heat treatment, the platelet/needle-like β-Fe phase undergoes partial dissolution during solution treatment at 500°C. Fig. 10 shows the presence of a large perforated platelet of the β-Al_5FeSi phase in M1 alloy following 24 h solution treatment at 500°C. These observations confirm the findings of Villeneuve *et al.* [23] on the fragmentation and dissolution of β-Al_5FeSi phase during solution

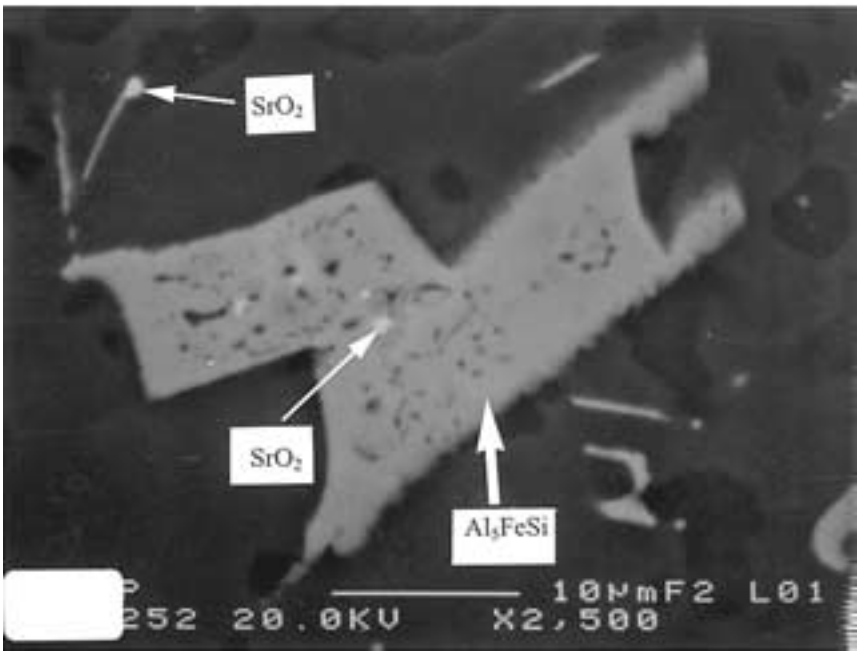

Figure 10 Backscattered image of the β-Al_5FeSi phase obtained from M1 alloy solutionized for 25 h at 500°C, showing perforation of the β-platelet. Note the presence of small white SrO_2 particles (arrowed).

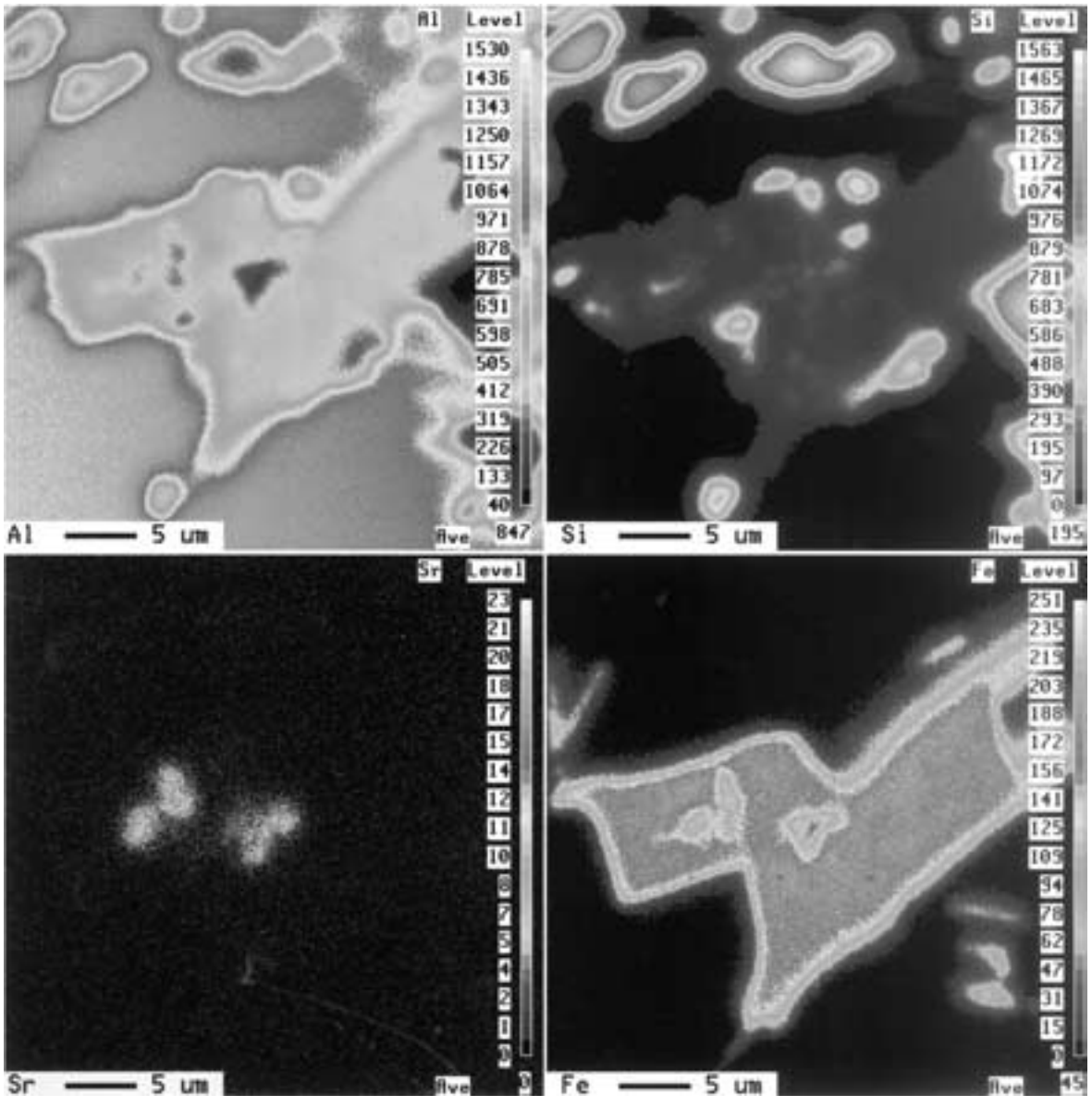

Figure 11 X-ray images of Al, Si, Sr, and Fe corresponding to the backscattered image of M1 alloy shown in Fig. 10.

Figure 12 Backscattered image of α-$Al_{11}(MnFeNiCu)_4Si$ script particles (arrowed) obtained from 2N alloy after 24 h solution heat treatment at 500°C.

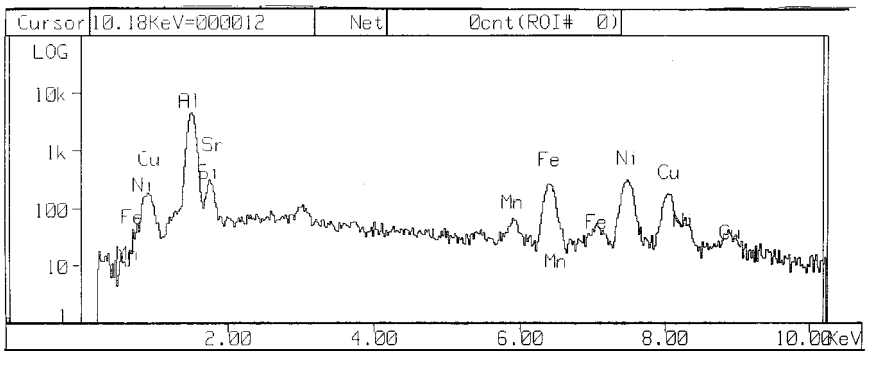

Figure 13 EDX spectrum corresponding to the α-$Al_{11}(MnFeNiCu)_4Si$ phase shown in Fig. 12.

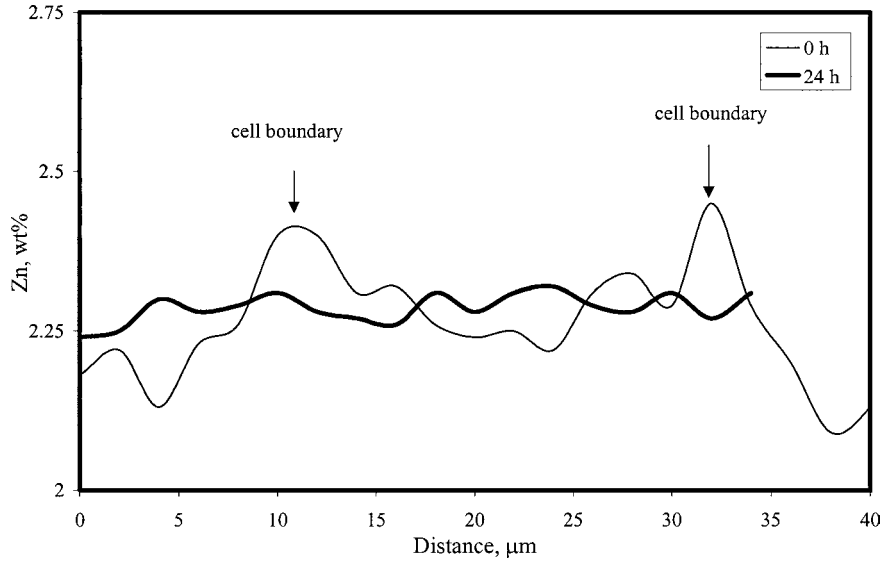

Figure 14 Zinc distributions obtained in Z alloy in the as-cast condition, and after 24 h solution treatment at 500°C.

heat treatment of Al-13 wt% Si-Fe alloys at 540°C. According to them, the dissolution of the β-phase occurs by decomposition of β-Al_5FeSi into Al_6Fe and Si particles.

In the present work on A413.1 alloy, the β-Al_5FeSi phase is expected to precipitate at 574°C during the Al-Si eutectic reaction (cooling rate ~0.8°C/s). As mentioned before, the maximum solution temperature was selected to be 500 ± 5°C, to avoid incipient melting of the copper phase. On account of this, decomposition of the β-Al_5FeSi phase may not fully take place. Instead, the β-Al_5FeSi plate surfaces are seen to contain perforations caused possibly by rejection of Si into the surrounding matrix [23].

From WDS analysis, the Fe:Si ratio (wt%) was found to vary between 21:9 and 18:14 across the width of the β-Fe platelet, confirming this possibility. For the analysis, six readings were taken to cover the platelet width, at intervals of 2 μm (corresponding to the size of the zone analyzed by the electron beam).

Fig. 11 shows the X-ray images of Al, Si, Sr and Fe of the β-Al_5FeSi phase shown in Fig. 10. As can be seen, the intensity of Fe is noticeably higher than that of Si throughout the β-Al_5FeSi platelet. Also, small particles of strontium oxide (SrO) are seen on the surface of the β-Al_5FeSi platelet, suggesting that these particles act as possible nucleation sites for the precipitation of the β-Al_5FeSi phase.

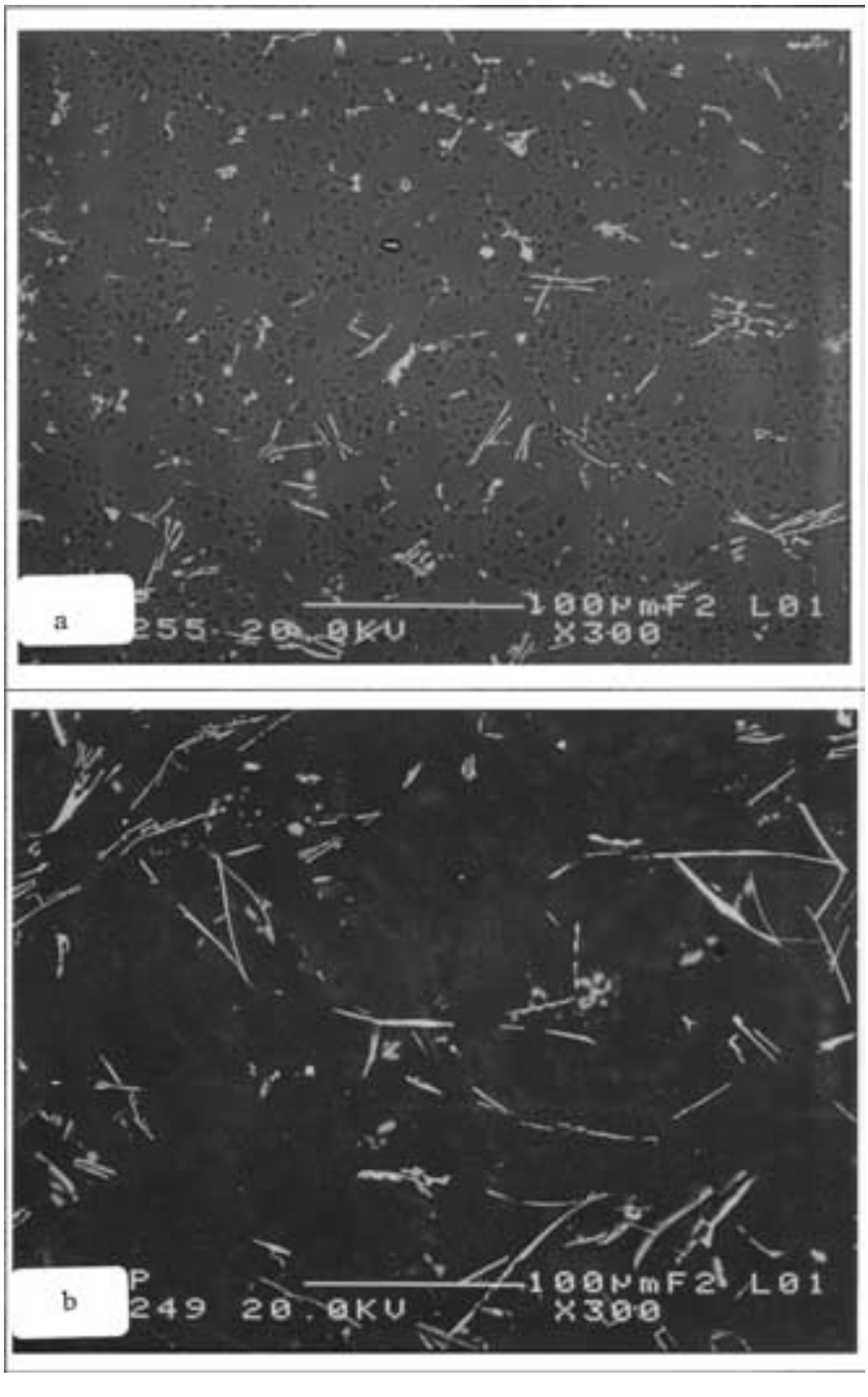

Figure 15 Low magnification backscattered images of (a) Z alloy and (b) M4 alloy solution heat-treated for 24 h at 500°C, showing the modification effect of Zn on the β-Al_5FeSi phase.

3.2.5. Ni-containing phases

Samples corresponding to the Sr-modified 2N alloy after solution treatment at 500°C for different times were examined microscopically. Fig. 12 is the backscattered micrograph obtained from 2N alloy solution heat-treated at 500°C for 24 h. It is clear that the Ni-containing α-$Al_{11}(MnFeNiCu)_4Si$ phase (arrowed) is stable, similar to the $Al_{15}(MnFe)_3Si_2$ phase. The composition of this phase in at% was determined to be 69 Al, 5 Cu, 6.6 Si, 6 Fe, 11.4 Ni, and 1.3 Mn from WDS analysis. Thus, it appears that increasing the number of elements and their amounts (in terms of number of atoms) in an intermetallic compound increases its stability during solution heat treatment. Fig. 13 is the corresponding EDX spectrum taken from an α-$Al_{11}(MnFeNiCu)_4Si$ particle, showing strong reflections due to Al, Mn, Fe, Ni, Cu, and Si elements.

3.3. Zn distribution

Copper, magnesium, silicon, and zinc are the principal solutes involved in precipitation hardening reactions and have relatively high rates of diffusion in aluminum. Rapid solidification is expected to produce minimum microsegregation across the dendrite cell walls. Since these cell walls are relatively small, uniform solute redistribution can be achieved upon homogenizing at 500°C. This is evident from Fig. 14, illustrating the Zn concentration distribution (wt%) before and after solution heat treatment for 24 h at 500°C. It should be note that Zn could as well lead to some modification of β-Al_5FeSi phase, as inferred from the backscattered image of Fig. 15a for Z alloy following 24 h solution treatment at 500°C (average β-platelet size $\sim$25 μm), compared to that obtained from the M4 alloy treated similarly, Fig. 15b (average β-platelet size $\sim$70 μm).

4. Conclusions

A study of the effect of Mg, Cu, Be, Ag, Ni and Zn alloying additions and solution heat treatment (at 500°C for times up to 24 h) on the microstructural characteristics of A413.1 alloy was carried out. From the results obtained the following was concluded.

1. Addition of 0.42% Mg to the unmodified eutectic Al-Si alloy results in large Si particles in the as-cast condition (DAS $\sim$22 μm). With increase in the solution treatment time, the Si particle characteristics (area, length, aspect ratio, roundness ratio and density) in the base A413.1 and Mg-containing alloys become approximately the same.

2. Both Mg_2Si and Al_2Cu phases in Al-Si alloys dissolve almost completely during solution treatment at 500°C for 8 h, or less.

3. The $Al_5Cu_2Mg_8Si_6$ and α-$Al_{15}(MnFe)_3Si_2$ (or α-Fe) intermetallic phases are insoluble during solution treatment at 500°C for times up to 24 h.

4. The plate-like β-Al_5FeSi phase (which may nucleate on SrO particles during solidification) partially dissolves during solution treatment through the diffusion of Si atoms into the surrounding matrix. However, this process may need more than 24 h at 500°C before it is completed.

5. Nickel and Cu dissolve in the α-$Al_{15}(MnFe)_3Si_2$ phase, contributing to its higher stability during solution treatment.

6. Addition of Zn in the presence of Sr further modifies the β-Al_5FeSi phase compared to that achieved with the addition of Sr alone (cf. average β-platelet sizes of 25 μm and $\sim$70 μm in the two cases following solution heat treatment at 500°C for 24 h).

Acknowledgements

Financial and in-kind support received from the Natural Sciences and Engineering Research Council of Canada (NSERC), General Motors Powertrain (U.S.A.), Corporativo NEMAK (Mexico), and the Centre Québécois de Recherche et de Développement de l'Aluminium (CQRDA) is gratefully acknowledged. The authors would also like to thank Mr. Glenn Poirier of the Microanalysis Laboratory, Earth and Planetary Science, McGill University for carrying out the EPMA analysis, and Dr. A.M. Samuel for a critical review of the manuscript. Also, Dr. M.A. Moustafa wishes to acknowledge the Central Metallurgical Research and Development Institute (CMRDI), Egypt for leave of absence.

References

1. TENG-SHIH SHIH and FANG-SHEA SHIH, *Int. J. Cast Met. Res.* **10** (1998) 273.
2. A. M. SAMUEL, P. OUELLET, F. H. SAMUEL and H. W. DOTY, *AFS Trans.* **105** (1997) 951.
3. H. DE LA SABLONNIÈRE and F. H. SAMUEL, *Int. J. Cast Met. Res.* **9** (1996) 195.
4. P. OUELLET, F. H. SAMUEL, D. GLORIA and S. VALTIERRA, *ibid.* **10** (1997) 67.
5. C. W. MEYERS, K. H. HINTON and J. S. CHOU, *Mater. Sci. Forum.* **102–104** (1992) 75.
6. D. APELIAN, S. SHIVKUMAR and G. SIGWORTH, *AFS Trans.* **97** (1989) 727.
7. S. SHIVKUMAR, C. KELLER, M. TRAZZERA and D. APELIAN, in Proc. Int. Symposium on Production, Refining, Fabrication and Recycling of Light Metals, Hamilton, Ontario, August 26–30 (1990), edited by M. Bouchard and P. Tremblay (Pergamon Press, New York, 1990) p. 264.
8. L. PEDERSEN and L. ARNBERG, *Metall. Mater. Trans.* A **32A** (2001) 525.
9. C. L. McADAM and D. C. JENKINSON, in Proc. 27th Annual Congress of the Australian Institute of Metals, Christchurch (1974) Vol. 27, p. 58.
10. P. S. WANG, S. L. LEE, J. C. LIN and M. T. JAHN, *J. Mater. Res.* **15** (2000) 2027.
11. Q. G. WANG and C. H. CACERES, *Mater. Sci. Forum* **242** (1997) 159.
12. M. A. MOUSTAFA, F. H. SAMUEL, H. W. DOTY and S. VALTIERRA, *Int. J. Cast Met. Res.* **14** (2002) 235.
13. S. SHIVKUMAR, R. RICCI, Jr. and D. APELIAN, *AFS Trans.* **98** (1990) 913.
14. L. F. MONDOLFO, "Aluminum Alloys: Structure and Properties" (Butterworths, London-Boston, 1976) p. 566.
15. F. H. SAMUEL, A. M. SAMUEL and H. W. DOTY, *AFS Trans.* **104** (1996) 893.
16. A. M. SAMUEL, J. GAUTHIER and F. H. SAMUEL, *Metall. Mater. Trans.* A **27A** (1996) 1785.

17. M. HANSEN, "Constitution of Binary Alloys," 2nd ed. (McGraw-Hill Book Co, New York, 1958) p. 84.
18. J. H. SOKOLOWSKI, X. SUN, G. BYCZYNSKI, D. O. NORTHWOOD, D. E. PENROD, R. THOMAS and A. ESSELTINE, *J. Mater. Proc. Techn.* **53** (1995) 385.
19. F. H. SAMUEL, *J. Mater. Sci.* **33** (1998) 2283.
20. O. REISO, H. G. OVERLIE and N. RYUM, *Metall. Trans.* A **21A** (1990) 1689.
21. J. H. SOKOLOWSKI, M. B. DJURDJEVIC, C. A. KIERKUS and D. O. NORTHWOOD, *J. Mater. Proc. Techn.* **109** (2001) 174.
22. L. BACKERUD, G. CHAI and J. TAMMINEN, "Solidification Characteristics of Aluminum Alloys," Vol. 2, Foundry Alloys, AFS/Skanaluminium (Des Plaines, IL, USA, 1990) p. 86.
23. C. VILLENEUVE and F. H. SAMUEL, *Int. J. Cast Met. Res.* **12** (1999) 145.

Received 23 July 2002
and accepted 16 January 2003